SCIENTIFIC PROBLEMS
OF MACHINES OPERATION
AND MAINTENANCE
4 (164) 2010

STANISŁAW ŚCIESZKA*, WOJCIECH GRZEGORZEK*,
MARCEL ŻOŁNIERZ*

Simulative tribo-testing of erosive wear for coal impact mills

Key words

Abrasion and erosion wear, grinding action.

Słowa kluczowe

Zużycie ścierne i erozyjne, proces mielenia.

Summary

In some lignite-fired power stations, very high wear appears in the impact mills and in related processing equipment such as classifier flaps, splitters, and fuel pipe bends. In the power industry, abrasion and erosion wear are important cost generating factors during the conveyance of raw coal, during the coal grinding process, during the conveyance of pulverised fuel, and during the conveyance of ash. Three laboratory methods were developed that require the use of three separate rigs to simulate the following: a) grinding action and erosion wear in the coal impact mills, b) classifier flap erosion wear by solid coal fuel particles impingement, and c) coal fuel pipe bends and splitters erosion wear.

Definition of problem

Very high wear appears in the coal pulverises and in related processing equipment such as classifier flaps, splitters, and fuel pipe bends at the lignite-fired power stations. The intensity of abrasion and erosion wear experienced in some impact mills is particularly severe. The impact mill presented on Figure 1

* Silesian University of Technology, Faculty of Mining and Geology, Institute of Mining Mechanisation, Akademicka 2A Street, 44-100 Gliwice, Poland; e-mail: stanislaw.scieszka@polsl.pl.

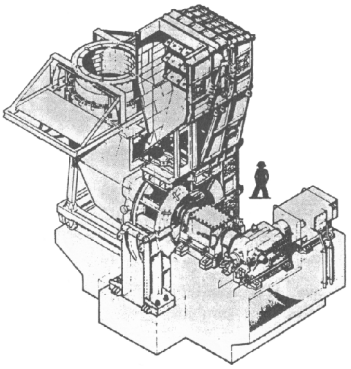

Fig. 1. Rotary impact mill
Rys. 1. Obrotowy młyn udarowy

is designed like a centrifugal fan with radial blades. Pulverisation is by impact on the blades and housing. The mill is basically a housing (mill case) inside which is a wheel with wear-protected blades. This wheel is fitted to a shaft that rotates at a speed according to the kind of mill. A static classifier is fitted at the top of the mill.

These mills are used principally for processing lignites, which are characterised by high moisture content. By means of a suitable supply of hot gas, the product is dried before being fed into the mill.

As it can be seen from the scheme in Figures 1 and 2, coal and the suspension medium (including that contaminated by the fly ash and hot air from the boiler) enter the mill axially and must change direction to a radial one.

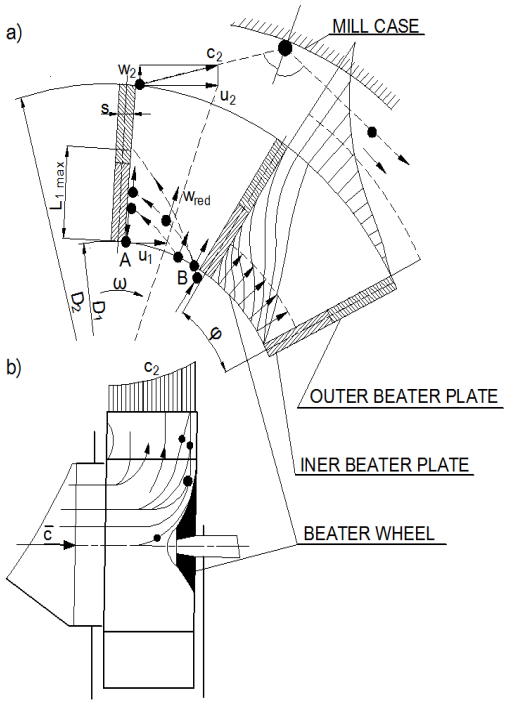

Fig. 2. Scheme of the rotary impact mill: a) Impact area of coal with the beater plate and mill case; b) Coal and suspension medium flow pattern inside the mill. Where: c – velocity distribution, $\bar{c}$ – mean velocity of coal and the suspension medium, D_1, D_2 – inner and outer diameter of the wheel, ω – angular velocity, u_1 – beater plate velocity at point A, u_2 – beater plate velocity at radius $r_2 = D_2/2$, c_2 – coal and suspension medium resultant velocity
Rys. 2. Schemat obrotowego młyna udarowego: a) Obszar oddziaływania węgla z płytą bijaka i obudową młyna, b) Model przepływu węgla i nośnika wewnątrz młyna. Gdzie: c – rozkład prędkości, $\bar{c}$ – średnia prędkość węgla i jego nośnika, D_1, D_2 – wewnętrzna, I – zewnętrzna średnica koła udarowego, ω – prędkość kątowa, u_1 – prędkość liniowa bijaka w punkcie A, u_2 – prędkość liniowa bijaka na promieniu $r_2 = D_2/2$, c_2 – prędkość wypadkowa węgla i nośnika

This is accomplished before entering the working beater wheel. The area of the impact of coal grains with the beater plate depends on the grain entry into the wheel. Theoretically, it can be at any point on the cylinder surface of the wheel of inner diameter D_1, limited by two adjacent plates and the inner width of the wheel. Nevertheless, due to the effect of inertial forces on the grains, the concentration of mass occurs in a third of the wheel width.

If the grains enter the wheel close to the plate of point A, impact on the plate edge (at diameter D_1) will take place. As the entry position translates from point A to B, the longer path directs the grains in a radial direction, while the beater plate approaches. In the region of D_1 to D_1+L_{1max} the inner beater plate will be subjected to the most intensive wear. Two specific types of abrasion-erosion can occur in this region: Gouging erosion, heavy plastic deformation of a surface by hard mineral fragments (e.g. quartz and pyrite) under impact causing deep surface grooving and removal of relatively large wear debris particles [1, 2]. The process is caused by mineral fragments under sufficient contact stress to cause the mineral fragments to fracture. The abrasion also takes the form of scratches on the contacted surface.

In the region up to D_2, the outer plate wear will be less intensive, since only sliding of the grains on the plate surface causes it. This wear is of a different depth, having a wavy appearance due to the effect of the secondary flow of the carrying medium (circulation, non-uniformity of speed profile). In this region, the predominant wear mode is low stress scratching abrasion (sliding-erosion). In this mode, wear occurs mainly by cutting or ploughing by a mineral fragments under contact stress below their crushing strength.

Grinding intensity depends mainly on the impact force of the grain contact with the beater plate and on the number of contacts. Impact force depends on impact speed. In the analysed mill, the peripheral speed was about 100 m/s.

Pulverised coal mixed with a part of combustion air is transported from the mill through the classifier and splitters along fuel pipes to boiler burners at a velocity of about 25m/s. Since the velocity of impacting particles is one of the important parameters governing solid particle erosion wear, the pulverised fuel system is designed to keep the velocity below the above-mentioned value. Then all elements of the pulverised fuel system are exposed to predominantly solid particle erosion wear, but in pipe bends it is more distinctly low angle impingement erosion and low stress scratching abrasion than in other cases [3, 4].

Characterisation of erosive particles

Particle characterisation for an assessment of the abrasion and erosion action must take into account the amount and the mode of the transfer of the kinetic energy of the particles to the worn surface. The energy stored in moving or stressed particles depends on the diameter and density at the points of contact between the particles and the target. Some of the potential or kinetic energy is first

utilised to deform and subsequently to remove material from the surface. The efficiency of the abrasion or erosion mechanism depends on the shape, hardness, and strength of the particles. Hard, high-strength, sharp-edged particles (e.g. quartz and pyrite) are able to transmit relatively high amounts of energy over small areas, thus causing rapid abrasion or erosion wear [5, 6].

The coal substance is a soft, low-strength material (Table 1); therefore, the wear-causing properties of different coals depend largely on the presence of abrasive mineral types (Figure 3).

Table 1. Concentration and hardness of coal constituents [4]
Tabela 1. Udział i twardość składników węgla

Constituent	Approximate concentration	Vickers hardness	Mohs hardness
	(weight percentage)	(kg/mm^2)	-
Soft minerals, Vickers hardness < 100kg/mm^2			
Coal substance	75	10-80	1.5-2.5
Kaolinite	5	30-40	2.0-2.5
Illite	3	20-35	2.0-2.5
Muscovite	3	40-80	2.0-2.5
Medium-hard minerals, Vickers hardness 100-600 kg/mm^2			
Calcite	0.5	100-170	3
Siderite	0.2	370-440	4
Magnesite	< 0.1	370-520	4
Ankerite	0.1	350-490	4
Dolomite	< 0.1	420-580	4
Hard minerals, Vickers hardness > 600 kg/mm^2			
Pyrite	1.5	720-1840	6-7
Quartz	1.5	1100-1560	7
Orthoclase	< 0.1	700-800	6
Kyanite	< 0.1	500-2100	5-8
Topaz	< 0.1	1500-1700	7-8
Alumina	Rare	>2000	9

Table 2. Hardness of coal mineral species and ash constituents
Tabela 2. Twardość składników węgla i popiołu

Species	Amount	Vickers hardness	Mohs hardness
	(weight ercentage)	(kg/mm^2)	-
Coal minerals			
Alumino-silicates	70	20-80	2-2.5
Quartz	15	1200-1300	7
Pyrite	10	1100-1300	6-7
Carbonate	5	150-450	3-4
Pulverised fuel ash			
Glassy spheres with embedded mullite needles and quartz crystalloids	80	550-600	5
Small glassy and large nonspherical quartz particles	10	600-1200	6-7
Spherical particles of iron oxide	5	480-740	5-6

The transformation of coal mineral matter to fly ash in pulverised fuel flames take place in a temperature range of 1700 to 1900K. High temperature and rapid heating cause marked changes in particle size, shape, and hardness (Figure 4 and Table 2); therefore, the flame-imprinted abrasive characteristics of fly ash can be significantly different from those of the original mineral matter. A highly abrasive coal mineral matter, rich in quartz, produces an abrasive ash in which the large quartz particles retain the wear-causing property. If the ash is recirculated with hot air from the boiler, it may considerably increase wear in mills. The scope for combating pulverised fuel and ash impact erosion and abrasion in existing milling systems is rather limited.

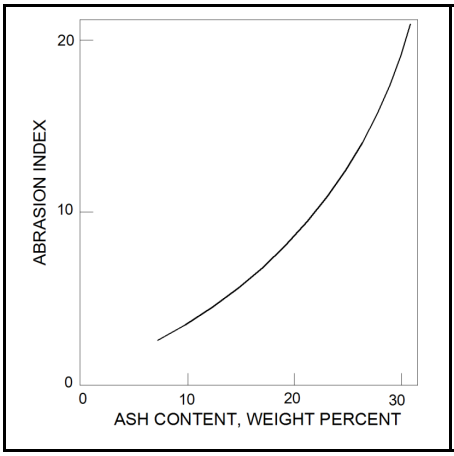

Fig. 3. Increase in abrasion index with ash content
Rys. 3. Wzrost wskaźnika ścieralności w zależności od zawartości popiołu

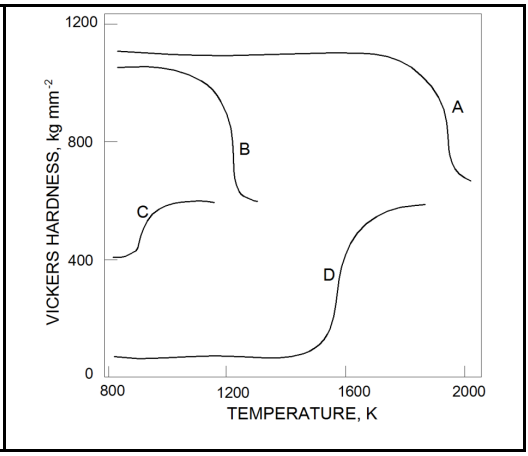

Fig. 4. Change in hardness of coal minerals on heating: A – quartz, B – pyrite, C – siderite, D – alumino-silicates, kaolin, illite
Rys. 4. Zmiana twardości składników węgla z temperaturą: A – kwarc, B – piryt, C – syderyt, D – glinowo-krzemowe, kaolin, illit

Characterisation of materials

In this part of the paper, assessment is made on possible major changes in the pulverised coal-fired system, and the main emphasis is put on possible material choice for the most intensively worn parts such as beater plates, splitters, and pipe bends.

The removal of material from surfaces by coal fragments or pulverised coal fuel is a complex process and varies in intensity depending on material microstructure, mechanical properties of various phases, the hardness of abrasive fragments, and size, shape, and the environment [7]. Removal of material during the abrasive wear processes can occur by cutting or by ploughing [1, 2]. The cutting process is much more efficient and results in more severe wear. The likelihood of cutting by abrasive particles increases with the

sharpness and angularity of the particles. Therefore, quartz particles crushed on the surface of the beater plate will be much more aggressive than other coal components. Since gouging abrasion-erosion normally occurs in the crushing of relatively large pieces of coal, the abrasive wear is usually accompanied by heavy impact and high bending or compressive stresses on the beater plates.

This imposes definite limitations on the choice of ferrous alloys that can be used without premature breakage in this service. Traditionally, the austenitic 12% manganese steels have been the prime choice for beater plates. They have fairly good resistance to gouging abrasion, combined with good toughness and the ability to be heat-treated in heavy sections. However, in some cases, the manganese steels have been at least partially displaced by low-alloy quenched and tempered steels and by martensitic white irons.

Zum Gahr [3] contends that abrasion resistance is influenced by the quantity of carbides in the metal part, the carbide morphology, retained austenite, internal notches, and the matrix structure. These structural components also influence the toughness of the part, something that must ultimately be considered when choosing the material for coal pulverising plates. In materials containing massive carbides, such as high-chromium cast iron, the mean free path between carbides in relation to abrasive particle size is significant to abrasion resistance. The following micro-structural features tend to improve abrasion/erosion resistance: small mean path between carbides, low interface energy, and the ratio of scratch width made by the abrasive to carbide size. In materials having a ferritic matrix with M_3C carbides, silica will penetrate and plough both the matrix and carbide. The M_3C carbide is not hard enough.

Carbides such as $(FeCr)_7C_3$ are much harder than silica and resist ploughing penetration. Pearlitic structures are easily disrupted by silica abrasion. The cementite is deformed and fractured and is torn out of the ferrite phase by the action of silica particles. Materials having massive, hard carbides supported in a relatively soft matrix will tend to wear by the extraction of the matrix material. This is true especially for high stress grinding or for gouging abrasion. There are indications [4] that corrosion plays a role in the wear of coal processing equipment.

The hardness and fracture toughness are very important mechanical properties that influence the abrasive and erosive wear resistance of materials such as high-chrome white cast irons, cast basalt, and high alumina ceramic.

Solid particle erosion is the predominant kind of wear in coal fuel splitters and pipe bends. Knowledge about the mechanism of solid particle erosion wear originates from single particle impingement. Multi-particle impingement, which is experienced in industrial conditions, involves complex phenomena, including a wide range of simultaneous incidence angles, particle interactions, particles embedded in the surface, etc. Several mechanisms of the erosion of materials have been proposed. Some of the main processes involved in erosion wear were summarised by Zum Gahr (Figure 5). Angular particles can remove material by microploughing and/or microcutting when

they strike the target surface at small angles. Temperature effects can be superimposed, due to high impact energies and friction forces induced by adhesion between the particles and the target. The ratio of particle hardness to the hardness of the target plays a role. The ranking order of hard and soft materials can be changed unfavourably in respect to the hard materials with the transition from low to high levels of solid particle erosion wear. Surface cracking becomes important with increasing impingement angle, particle size, particle velocity, and the increasing brittleness of the target material. Erosion rates were observed to be substantially more sensitive to particle size on brittle than on ductile materials (Appendix A).

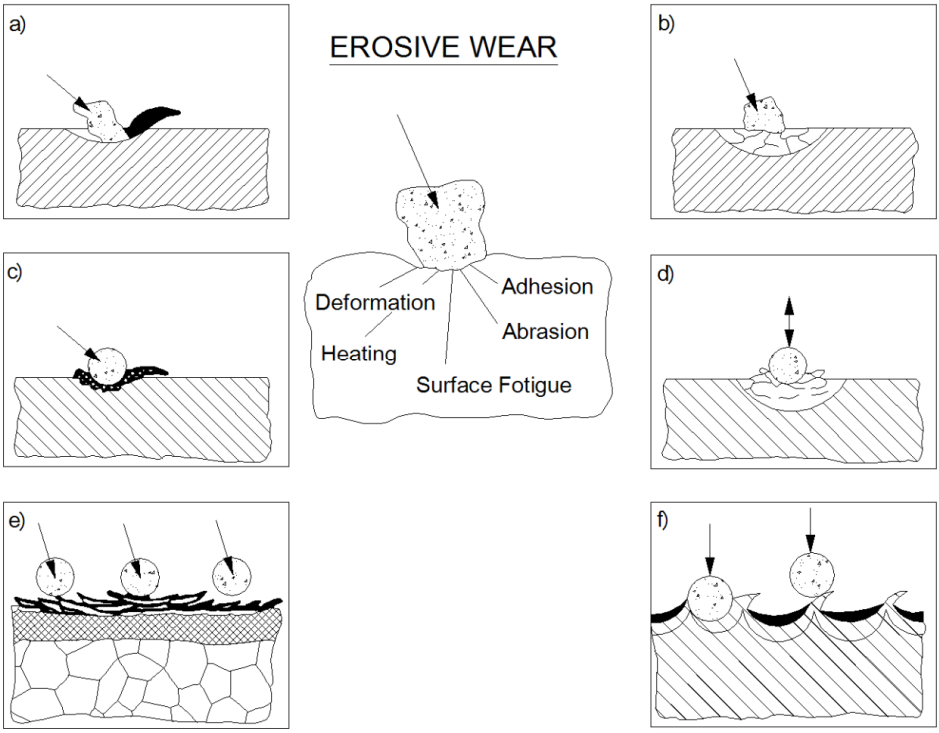

Fig. 5. Processes resulting in wear loss due to single or multiple impact of particles [4]. Where: a) microcutting and microploughing, b) surface cracking (microcracking), c) extrusion of material at the exit end of impact craters, d) surface and subsurface fatigue cracks due to repeated impact, e) formation of thin platelets due to extrusion and forging by repeated impact, f) formation of platelets by a backward extrusion process

Rys. 5. Procesy prowadzące do zużycia z powodu pojedynczego lub wielokrotnego uderzenia cząstek. Gdzie: a) mikroskrawanie i mikrobruzdowanie, b) pęknięcia powierzchniowe (mikropęknięcia), c) wyciskanie materiału na wyjściu z kraterów, d) powierzchniowe i podpowierzchniowe pęknięcia zmęczeniowe z powodu powtarzającego się uderzenia, e) powstawanie cienkich płytek z powodu wyciskania i kucia przez powtarzające się uderzenia, f) powstawanie płytek przez proces wyciskania przeciwbieżnego

The mass loss due to erosion was reported to be proportional to about the square of the velocity of the cause of ductile materials (Appendix A). However, substantially greater velocity exponents up to 5 were reported on brittle materials such as ceramics. Material lips can be produced by oblique impact and are finally detached along shear bands.

Repeated loading cycles by the multiple impact of particles provide the formation of surface or subsurface cracks, which lead finally to the flaking of wear debris. The formation of thin platelets (Figure 5) is favoured by the multiple impact of rounded particles under high angles of incidence. In practice, several of these wear processes can occur simultaneously, depending on the operating conditions and the target material.

Target material properties such as hardness, work hardening, and the capability of deformation, are important physical properties for its resistance to solid particle erosion. Dynamic hardness and work hardening of the target determine the amount of plastic deformation and hence the depth of impact craters at a given impact energy and angle of incidence. The capability of the deformation of the metal during impact loading affects the number of impacts that are required for the formation of wear debris. As a result, a softer metal can show greater erosion resistance than a harder one. Temperature effects can influence wear mechanisms substantially, due to altered microstructures and properties with increasing impact energy or ambient temperature. Chemical effects may be superimposed, depending on the environment (Appendix A).

Experimental testing

Test equipment

It was recognised that the problem of excessive wear is concentrated in three separate parts of the mill system:

a) The rotating impact beater plate,
b) The classifier flaps, and
c) The pipe bends.

Each of these areas is characterised by a different wear mechanism, and the applied testing methods are based on three separate experiments:

1) Simulation of impact abrasion-erosion on the beater plates using raw lignite;
2) Simulation of classifier flap erosion by solid particle erosion using pulverised fuel; and,
3) Simulation of the wear on the pipe bends by means of the spinning erosion wheel.

It is assumed that the problem of the excessive wear is due to the incorrect selection of the material and the aim of the experiments was to find more appropriate materials in each case, although the problem appears to be

compounded by the abrasive quality of the coal and the high recirculation rate of ash. For every three experiments, separate rigs were designed and built.

Experiment 1. Impact-abrasion rig is shown in Figure 6.

Experiment 2. The solid particle erosion equipment was built according to the ASTM designation G76-83 recommendation. The rig is shown in Figure 7.

Experiment 3. Spinning wheel for pipe bend wear is shown in Figure 8.

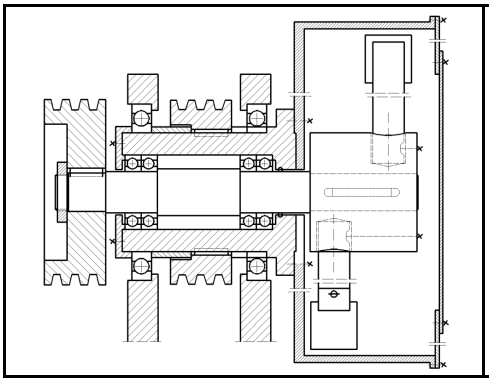

Fig. 6. Schematic drawing of impact-abrasion Equipment, with impact speed $v_i = 100$ m/s
Rys. 6. Schematyczny rysunek urządzenia do badania ścierania udarowego, z prędkością uderzenia $v_i = 100$ m/s

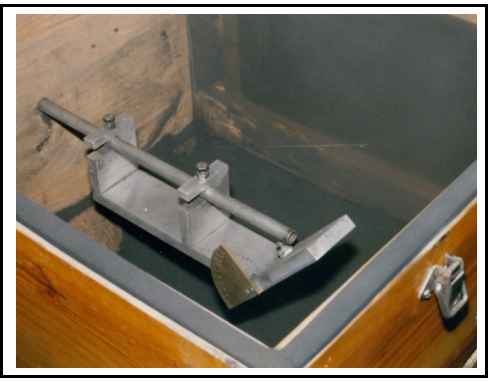

Fig. 7. Erosion tester, nozzle tube and specimen holder
Rys. 7. Tester do badania erozji, dysza i uchwyt próbki

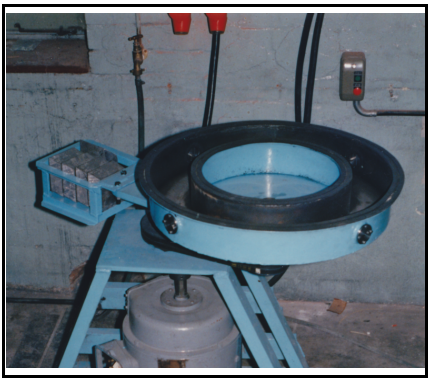

Fig. 8. Overall view of the spinning erosion wheel
Rys. 8. Ogólny widok wirującego koła do badania erozji

Coal and pulverised fuel identification

For abrasion-erosion tests, raw and pulverised lignite from a selected power station were used. Comparison between the raw and pulverised lignite indicates that the ash content is 4-6% higher in the pulverised products than in the raw

lignite [6]. This confirms that additional ash is fed in from the furnace during the grinding process. The hardness of the fly ash and the minerals is considerably higher than that of coal, as tested by microhardness methods [6].

Table 3. Lignite analysis
Tabela 3. Analiza węgla brunatnego

Analysis	Raw Lignite	Pulverised Fuel Upperduct	PF Product
Proximate:			
Moisture %	7.6	8.9	7.7
Volatile %	36.4	32.3	33.3
Ash %	33.6	38.7	40.5
F.C % (by diff.)	22.4	20.1	18.5
Free Silica ($Si0_2$ % in ash)	6.4	6.1	5.8

Experimental results

Simulation of impact-abrasion on the beater plates using raw lignite

In all tests, raw lignite samples were used, M = 500 g. Other test data:

1. Test duration, t = 5 min.
2. Drum rotation, $n_1 = 3\ 000\ min^{-1}$.
3. Paddle rotation, $n_2 = 3\ 000\ min^{-1}$.
4. Distance between paddle and drum d = 2mm.

Measurements taken:

1. Mass of specimens before test, m_1, g.
2. Mass of specimens after test, m_2, g.
3. Mass lost during test, Δm, g.
4. Pulverised coal during test, fraction below 212μm, PC, g.

Erosion wear was calculated as erosion factor (*EF*)

$$EF = \frac{\Delta m}{M} \cdot 10^6, \qquad \frac{mg}{kg} \tag{1}$$

Hence, relative erosion resistance (ε) was calculated for all materials tested assuming that for the least erosion resistance materials ε = 1.

Final results from these experiments are summarised in Table 4.

Table 4. Results from impact-abrasion experiments
Tabela 4. Wyniki badań ścierania udarowego

No	Material	*EF* mg/kg	ε -
1	25% Cr Cast Iron (Martensitic)	51.72	14.20
2	25% Cr Cast Iron (Austentic)	78.60	9.35
3	12% Cr Tool Steel	275.90	2.66
4	12% Mn Steel	510.30	1.44
5	12% Mn Steel (Highveld)	540.20	1.36
6	High Carbon Tool Steel	734.90	1.00

The experimental results allow the materials to be classified according to their resistance to the type of wear mechanisms which take place on the beater plates. The predominant mechanisms are gouging erosion (front face of specimens) and low-stress scratching abrasion (external side of the specimens).

The results indicate that the life expectancy of the beater plate could be increased by up to 14 times by using the 25 percent chrome cast iron instead of the carbon tool steel originally used or by a factor over 2.6 by using the 12 percent chrome steel.

Simulation of classifier flap erosion by solid particle erosion test using pulverised fuel from a power station

The erosion of classifier flaps in pulverised-fuel lines can be most closely modelled by a particle-gas stream type erosion tester. Erosion tests were performed using the apparatus illustrated in Fig 7. A predetermined mass of pulverised fuel (particle size below 212 μm) from the power station, M = 1 kg was fed into the air stream by means of a vibratory particle feeder. The concentration of particles was kept as close as possible to 1kg/h, although minor fluctuations occurred. The target was cleaned ultrasonically in alcohol, dried, and weighed on a 5-point balance both before and after testing (m_1, m_2). The particle velocity was kept constant (30 ms^{-1}) and was measured using the rotating double disc method developed by Ruff and Ives [7].

Three angles of impingement were used 30°, 60°, and 90°. Scanning electron micrographs were taken for surface examination and erosion mechanism interpretation (Fig. 9). The erosion rate (ER) was finally calculated by equation

$$ER = \frac{m_1 - m_2}{M} \cdot 10^3, \qquad \frac{mg}{kg} \tag{2}$$

Results are presented in Table 5.

Table 5. Summary of solid particle erosion experiment
Tabela 5. Podsumowanie eksperymentu erozji cząstek stałych

No	Target Material	*ER* mg/kg			$\overline{ER}$ mg/kg
		30º	60º	90º	
1	WC-7Co Binder	0.21	0.51	0.02	0.24
2	High Alumina Ceramic	0.42	0.38	0.40	0.40
3	25% Cr Cast Iron (Martensitic)	0.32	1.11	0.78	0.74
4	25% Cr Cast Iron (Austentic)	0.74	1.28	0.61	0.88
5	12% Cr Tool Steel	1.13	1.51	1.76	1.47
6	Roqlast	1.76	2.32	1.47	1.52
7	Mild Steel 43A	1.33	1.92	1.49	1.58
8	High Alumina Ceramic	0.90	2.88	1.49	1.76
9	High Carbon Tool Steel	1.31	2.66	1.32	1.76
10	12% Mn Steel	1.26	2.36	1.72	1.78
11	12 Mn Steel (Highveld)	1.74	2.66	1.92	2.11
12	Cast Basalt	3.87	4.40	5.98	4.75
13	Epoxy System	33.08	23.68	23.58	24.78

The solid particle erosion test allows the materials for the classifier flaps to be evaluated according to their resistance to erosion by pulverised fuel particles. The experiments revealed that instead of 12% Cr tool steel 25% Cr cast iron (martensitic) could be used with almost double durability. The two most erosion resistant materials, namely hardmetal WC-7Co and high alumina ceramic, are both too expensive and too brittle for this type of application. It is quite significant that "Epoxy System" and "Cast Basalt" are both at the bottom of the ranking.

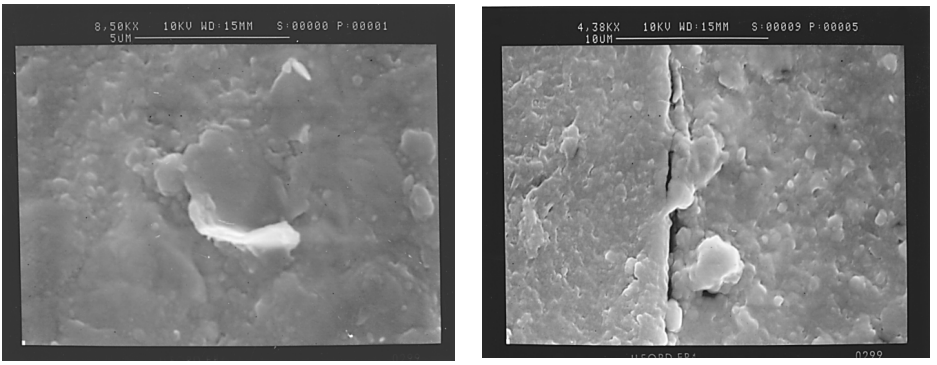

Fig. 9. Extrusion of matrix of the exit end of impact crater and fatigue crack propagation along carbide-matrix interface due to multiple impact on 25% Cr Cast Iron (martensitic)
Rys. 9. Wyciskanie osnowy na wyjściu z krateru i propagacja pęknięć zmęczeniowych na granicy fazy węglika i osnowy z powodu wielokrotnego uderzania na żeliwie stopowym 25% Cr (martenzytycznym)

In order to estimate the difference in the erosiveness between pulverised fuel (PF), which is contaminated by ash, and raw lignite (RAL), the same solid particle erosion procedure was applied using aluminium 6063 as a target specimen. Results are presented in Table 6.

Table 6. Results from comparative erosion test with pulverised and raw coal and aluminium as the target material

Tabela 6. Wyniki porównawcze badania erozji pyłu węglowego i węgla surowego oraz aluminium jako materiał tarczy

Test No	Particle type	Angle of impingement	m_1 g	M_2 G	ER mg/kg
1	PF	60º	6.88198	6.88083	1.15
2	RAL	60º	6.88083	6.88028	0.55
3	RAL	60º	6.88028	6.87928	0.65
4	PF	60º	6.87963	6.87850	1.13
5	PF	90º	6.58895	6.58842	0.53
6	PF	30º	6.59842	6.58627	2.15
7	RAL	90º	6.58461	6.58419	0.42
8	RAL	30º	6.58627	6.58461	1.66

Results indicate that pulverised fuel (PF) from the power station is substantially more erosive than raw lignite (RAL). The mean values of the erosion rate (ER) for PF and RAL are equal to 1.24 mg/kg and 0.82 mg/kg, respectively. As the scanning electron microscope study shows in Figs 10 and 11, this is due to the presence of sharp and hard ash particles in PF.

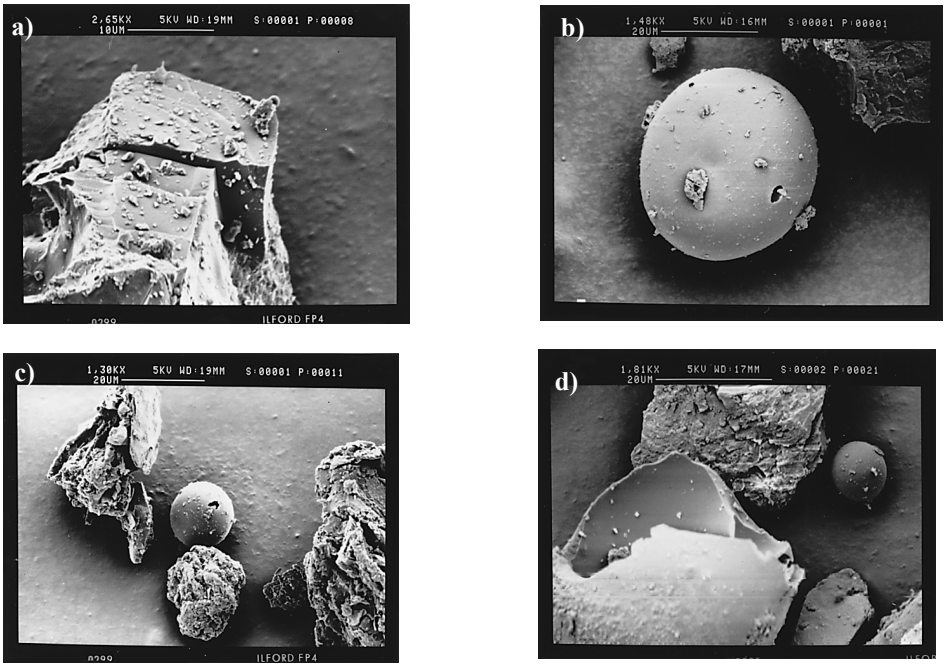

Fig. 10. Scanning electron micrographs showing characteristics feature of mineral particles and flame-heated silicate ash particles in pulverised fuel flame from power station: a) sharp-edged mineral particle; b, c) spheroidized flame-heated silicate ash particle; d) flame ash particle, broken cenosphere

Rys. 10. Mikrofotografie elektronowe skaningowe pokazują cechy charakterystyczne cząstek minerału i nagrzewanych płomieniowo cząstek pyłu żużlowego z elektrowni: a) cząstki minerału posiadające ostrą krawędź; b, c) kuliste wydzielenia nagrzewanych płomieniowo cząstek pyłu żużlowego; d) pęknięte cenosfery pochodzące z popiołu

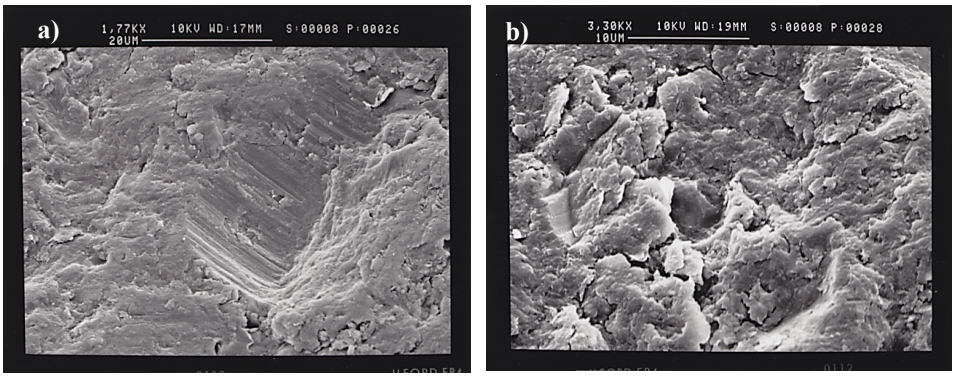

Fig. 11. Scanning electron micrographs showing aluminium target surface after erosion test: a) cutting as result of single impact of sharp particle; b) indentation and surface cracking due to multiple impact
Rys. 11. Mikrofotografie elektronowe skaningowe pokazują aluminiową powierzchnię tarczy po badaniu erozji: a) skrawanie w wyniku pojedynczego oddziaływania ostrej cząstki; b) wgniecenie i pęknięcie powierzchni z powodu wielokrotnego oddziaływania

Simulation of the erosion on the pipe bends by means of spinning erosion loop

The erosion in pipe bends was simulated in the spinning erosion loop (Fig. 8). In order to get uniform and accelerated results, silicon carbide particles (mark 100, 149 μm) were used. In every test, a mass (M = 1 kg) of silicon carbide was kept inside the wheel. The target specimen was cleaned ultrasonically in alcohol, dried and weighed on a 4-point balance both before and after testing (m_1, m_2).

The particle velocity against target was 10 ms^{-1}. Erosion intensity (EI) was calculated using the following equation:

$$EI = \frac{m_1 - m_2}{S \cdot t} \cdot 10^6, \qquad \frac{g}{m^2 h} \tag{3}$$

where:

S – surface area exposed to erosion, mm^2

t – duration of test, h

Erosion intensity (EI) represents the mass loss from a square meter of pipe bend surface during one hour of erosion action. Results are presented in Table 7.

Table 7. Summary of results from pipe bonds erosion tests
Tabela 7. Podsumowanie wyników z badań erozji na łukach rur

No	Target Material	*EI* G/m^2 h	ε -
1	WC - 7Co Binder	2.33	18.80
2	25% Cr Cast Iron (Austenitic)	3.75	11.70
3	High Alumina Ceramic No 1	4.22	10.40
4	25% Cr Cast Iron (Martensitic)	4.29	10.20
5	12% Cr Tool Steel	4.77	9.20
6	High Alumina Ceramic No 2	10.00	4.40
7	12% Mo Steel	10.76	4.08
8	High Carbon Tool Steel	10.78	4.07
9	12% Mn Steel	11.22	3.90
10	Roqlast	17.59	2.50
11	Cast Basalt	22.56	1.90
12	Epoxy System	24.60	1.80
13	Mild Steel 43A	43.90	1.00
14	Aluminium 6063	50.30	0.87

For materials ranking from this part of the research, the relative erosion resistance (ε) was used (Table 7). Relative erosion resistance was calculated assuming that, for material currently used for pipeline production (mild steel) ε = 1. Experiments show that a number of materials have higher erosion resistance than the mild steel. It is recommended that the pulverised fuel pipeline should be protected by means of internal sleeves made of 25% Cr cast iron (ε = 10.2 and ε = 11.7) or 12% Cr tool steel (ε = 4.07) or by tiles made of high alumina ceramic (ε = 10.4).

Conclusions and recommendations

1. The high speed impact-abrasion experiment enabled the materials to be classified according to their resistance to the kind of wear which is taking place on the beater plates surface. Results presented in Table 4 suggest that the life expectancy for the beater plates can be increased up to 14 times using 25% Cr cast iron (martensitic) instead of high carbon tool steel or over 2.6 times by applying 12% Cr tool steel. It is therefore recommended that 25% Cr cast iron be used for the inner beater plate, and 12% Cr tool steel be used for the outer plate, if fracture toughness data and cost consideration justify it.

2. The solid particle erosion experiment simulating classifier flaps wear revealed that the only materials which are significantly more resistant to erosion are 25% Cr cast iron (two times) and high alumina ceramic (four times).

Hardmetal WC-7Co is too expensive to be considered for this application. It is recommended that 25% Cr cast iron be used to make classifier flaps or high alumina ceramic tiles to protect classifiers made of mild steel.

3. Experiments simulating wear conditions on the pipe bends show that a number of materials have higher wear resistance than mild steel which is usually used for pipe production. It is recommended that the pulverised fuel pipeline should be protected by means of internal sleeves made of 25% Cr cast iron or 12% Cr tool steel or by internal tiles made of alumina.

References

[1] Moore M.A.: Abrasive Wear. Fundamentals of Friction and wear of Materials. ASM Materials Science Symposium, 1981, pp. 73-118.
[2] Murray M.J., Mutton P.J., Watson J.D.: Abrasive Wear Mechanisms in Steels. Journal of Lubrication Technology, Vol. 104, 1982, pp. 9-15.
[3] Zum Gahr K.H.: Mircostructure and Wear of Materials. Elsevier, Amsterdam 1987.
[4] Bakker W.T.: Evaluation of Coal Pulverizer Materials. EPRI Research Project Report 1883-2, Palo Alto, 1988.
[5] Skorupa J.J.: Wear of Tube Mill Liners for South African Power Industry. PhD thesis Cape Town. 1989.
[6] Falcon R.M.: Report on an investigation into Abrasion and Wear in Mills and Associated Plant in Amynteon Power Station. September 1989.
[7] Ruff A.W., Ives L.K.: Measurement of solid particle velocity in erosive wear. Wear, Vol. 35 (1975) pp. 195-199.

APPENDIX A

A review of erosion by solid particles

The erosion of materials resulting from the impingement of solid particles is one form of wear that can severely limit of useful life of an element of power plant fuel systems. Erosion can lead to rapid, significant loss of material under certain conditions such as coal processing in power stations under corrosive conditions at elevated temperature [1, 9-11].

Extensive plastic shear is necessary before metal removal occurs but it was not specified when erosive metal loss occurs. A model of steady-state erosion should explain the following general observations, which are expressed in terms of the dimensionless erosion rate, ER (e.g. milligrams of target loss per kg of abrasive).

1. ER varies as $(\text{velocity})^n$ where n is usually in the range from 2.2 to 5.0.
2. A maximum in the erosion rate for ductile metals is at an impact angle of 15° to 30°, or in the case of hardened steel maximum of 60° to 90°.

3. At low impact velocity (v) an incubation time is observed to be inversely proportional to v.
4. Particle size was found to have a significant influence on the erosion of pipe bends [2]. The authors found that sand particle of 70μm mean diameter wore the bends into a pattern of steps or ridges, whereas the 230μm diameter sand particle produced a smooth and round surface. Mills et al [3] found that 70μm particle removed less material that the 230μm particle.
5. Hardness of particles, there is widely held opinion that hard particles are more erosive than softer particles [4, 5].
6. Synergistic effects in erosion. Although the impacting particles used in erosion tests are usually pure and dry, in practice such as impact coal mills the particles are impure, and contain moisture. Small percentages of $Ca(OH)_2$ and water present in abrasives acted as effective intensifier of the erosive wear of metals and alloys [6]. However, with hard and high strength materials such as ceramics, the influence of impurities on erosion was found to be either very low, or to result in less damage.
7. Ruff and Wiederhorn erosion model. Wiederhorn and Lawn [7, 8] assumed that all the kinetic energy of the impinging particle is dissipated in an irreversible plasticity process and thus the following expression for ER was obtained:

$$ER = \alpha H^{0.11} V_0^{2.4} K_C^{-1.3} \rho_p^{1.2} R_p^{3.7}$$

Where: α – constant,
H – hardness of the target material,
V_0 – the particle velocity,
K_C – the fracture toughness of the target material,
ρ_p – density of the impacting particle,
R_p – particle radi

8. Thermal effects in erosion. A substantial temperature rise in the target accompanying an impact. Melting was postulated [7] as playing a significant role in metal loss. Heat is generated in the surface layer in two ways, by surface friction, and by lattice deformation. The tendency to surface melting depends primarily on flow stress, friction coefficient, and the heat required to raise the metal to its melting point, but not on the velocity. The impact of an eroding particle is so quick that the heat generated by deformation does not have time to diffuse away during the impact, provided the particles are over roughly 50μm in diameter [8]. If the surface is initially flat so that the deformation is distributed rather uniformly, the temperature rise is roughly 20-200°C. If the surface is uneven, the temperature rise may be much greater in the asperity struck first. Finally it may be stated that the local temperature

rise plays a critical role in creating the instability that gives the observed extrusion of near surface layer into lips.

References

[1] Shewmon P., Sundarajam G.: The erosion of metals. Ann. Rev. Sci. 1983, 13, pp 301-318.
[2] Mills D., Mason J. S. (1977): Particle size effects in bend erosion. Wear 44, pp. 311-328.
[3] Mills D., Mason J. S., Tong K. N. (1983): The role of penetrative wear in the erosion of pipe bends. Proceedings of the 6th International Conference on Erosion by Liquid and Solid Impact, pp. 58.1-58.7.
[4] Raask E. (1969): Tube erosion by ash impaction. Wear 13, pp. 301-315.
[5] Raask E. (1979): Impact erosion wear caused by pulverized coal and ash. Proceedings of the 5th International Conference by Solid and Liquid Impact, pp. 41-1 - 41-7.
[6] Uuemois H., Kleis I. (1975): A critical analysis of erosion problems which have been little studied. Wear 31, pp. 359-371.
[7] Jennings W. H., Head W. I.: Wear, 40 (1976), pp. 90-112.
[8] Shennon P.G.: Wear, 68 (1981), pp. 253-258.
[9] Hutchings I. M.: Tribology, Friction and Wear of Engineering Materials, Arnold, London, 1992.
[10] Stachowiak G. W. and Batchelor A. W.: Engineering Tribology, Butterworth-Heinemann, Woburn, 2001.
[11] Neale M. J. and Gee M.: Guide to Wear Problems and Testing for Industry. Professional Eng. Publ., London, 2000.

Scientific work executed within the Strategic Programme "Innovative Systems of Technical Support" for Sustainable Development of Economy Operational Programme.

Badania symulacyjne zużycia erozyjnego w węglowych młynach udarowych

S t r e s z c z e n i e

W niektórych elektrowniach opalanych węglem brunatnym pojawia się bardzo duże zużycie w młynach udarowych i związanych z nimi urządzeń, takich jak klapy sortownika, łupiarki i łuki przewodów paliwowych. W przemyśle energetycznym zużycie ścierne i erozyjne są ważnymi czynnikami generującymi koszty podczas transportu węgla surowego, podczas procesu kruszenia węgla, podczas podawania sproszkowanego paliwa do kotłów i podczas transportu popiołu. Opracowano trzy laboratoryjne metody badawcze oraz trzy odrębne testery: a) symulujący proces mielenia i zużycie erozyjne w węglowych młynach udarowych, b) symulujący zużycie erozyjne klap sortownika przez udar cząstek stałych paliwa węglowego, c) symulujący zużycie erozyjne na łukach przewodów paliwa węglowego oraz na rozdzielaczach.